

Challenging Λ CDM: 5σ Evidence for a Dynamical Dark Energy Late-Time Transition

Mateus Scherer,^{1,*} Miguel A. Sabogal,^{1,†} Rafael C. Nunes,^{1,2,‡} and Antonio De Felice^{3,§}

¹*Instituto de Física, Universidade Federal do Rio Grande do Sul, 91501-970 Porto Alegre RS, Brazil*

²*Divisão de Astrofísica, Instituto Nacional de Pesquisas Espaciais,
Avenida dos Astronautas 1758, São José dos Campos, 12227-010, São Paulo, Brazil*

³*Center for Gravitational Physics and Quantum Information,
Yukawa Institute for Theoretical Physics, Kyoto University, 606-8502, Kyoto, Japan*

Recently, there has been considerable debate regarding potential evidence for the dynamical nature of dark energy (DE), particularly in light of Baryon Acoustic Oscillations (BAO) measurements released by DESI survey. In this work, we propose an agnostic test that simultaneously constrains the dark energy (DE) equation of state (EoS) and probes the possibility of a transition between the quintessence and phantom regimes, or vice versa. Our initial approach is independent of physical priors, allowing the data to determine which behavior best fits the parameters. We then consider a minimally modified gravity theory known as VCDM, into which we can map our initial approximation, placing it within a theoretically stable framework. To this end, we incorporate the most up-to-date datasets available, including BAO measurements from DESI-DR2, Type Ia Supernovae from the PantheonPlus, DESY5, and Union3 samples, as well as Cosmic Microwave Background (CMB) data from Planck. Our analysis reveals strong and statistically significant evidence for a quintessence-phantom transition across various data combinations. *The strongest evidence is found for Planck+DESI+DESY5, with a significance exceeding $\sim 5\sigma$ in favor of a quintessence-phantom transition at $z_t = 0.493^{+0.063}_{-0.081}$.* Beyond this redshift, the EoS remains within the phantom regime, while for $z < z_t$, it favors the quintessence regime. Despite this strong indication, *we find that such transitions do not resolve the H_0 tension.*

I. INTRODUCTION

The standard cosmological model, known as the Λ CDM model, has been remarkably successful in explaining a wide range of cosmological observations over recent decades [1–6]. However, with the increasing precision of modern observations, several discrepancies have emerged that challenge the Λ CDM framework. The most prominent of these is the so-called Hubble tension [7–23], which refers to the discrepancy in the measurement of the Hubble constant H_0 . Local measurements, including those from Cepheid variable stars and Type Ia supernovae, provide values of H_0 that are significantly higher than those inferred from the Cosmic Microwave Background (CMB) data assuming the Λ CDM model, with the discrepancy reaching a significance greater than 5σ [7, 11].

In addition to the ongoing debate surrounding the Hubble tension, another key challenge in modern cosmology is the discrepancy in the parameter S_8 . This parameter, defined as $S_8 = \sigma_8 \sqrt{\Omega_m}/0.3$, relates the amplitude of matter fluctuations to the total matter density Ω_m . Early analyses of cosmic shear measurements suggested a tension exceeding 3σ [24, 25], but recent results from the KiDS survey indicate strong consistency with the Λ CDM model [26, 27]. Similarly, constraints on S_8 derived from ACT-CMB data align well with Planck-CMB predictions, further reinforcing the standard cosmological scenario [28]. Other observational probes also

support Λ CDM at the S_8 level [29–33]. However, full-shape analyses of large-scale structure data reveal a more significant tension, at the level of at least 4.5σ [34, 35], suggesting a potential discrepancy between early- and late-time universe constraints. Moreover, studies based on Redshift-Space Distortions (RSD) have also pointed to deviations that may indicate additional inconsistencies [36, 37]. Further observational probes have reported evidence of possible tensions in S_8 as well [38, 39]. The persistence of these discrepancies across various datasets raises important questions about the completeness of the Λ CDM model, potentially requiring modifications such as refinements in the modeling of the matter power spectrum, alternative DE scenarios, modifications to gravity, or interactions in the dark sector (see [40] for a general review).

On the other hand, observational efforts aimed at investigating the possibility of a late-time cosmological transition have long garnered interest—both as a probe of the fundamental nature of DE and as a potential resolution to the H_0 tension (see, for instance, [41–57]). Therefore, possible transitions in the dynamics of the universe related to the nature of dark energy have long been of great interest for observational tests.

From a recent observational standpoint, the Dark Energy Spectroscopic Instrument (DESI) has played a pivotal role [58, 59]. DESI is a state-of-the-art spectroscopic survey designed to map the large-scale structure (LSS) of the Universe in three dimensions, covering an extensive area of the sky across a wide redshift range. DESI has become the largest spectroscopic dataset of its kind to date, incorporating observations of millions of galaxies and quasars. This unprecedented dataset enables the

* mateus.scherer@ufrgs.br

† miguel.sabogal@ufrgs.br

‡ rafacnunes@gmail.com

§ antonio.defelice@yukawa.kyoto-u.ac.jp

construction of detailed 3D maps of the cosmic web, facilitates precise measurements of the Universe's expansion history [60, 61], and provides robust constraints on the dark energy equation-of-state (EoS) parameter [62, 63]. Additionally, the data support a wide array of cosmological analyses [64–87].

This paper investigates the possibility of late-time transitions in DE EoS. We propose an agnostic, data-driven test to probe whether DE undergoes a transition at low redshifts, characterized by a critical redshift z_{\dagger} . A key feature of our approach is that it does not rely on prior assumptions about the dynamics or physical nature of the EoS, thereby enabling purely observational constraints on whether the transition behaves like quintessence or phantom energy. We consider both abrupt and smooth transition models, with the latter motivated by the Lagrangian of a type II minimally modified gravity theory known as VCDM [88, 89]. In what follows, and throughout the discussion of our main results, we refer to these two approaches as w_{\dagger} CDM and w_{\dagger} VCDM, respectively. Both frameworks are employed in all our statistical analyses, with a mathematically equivalent smooth version developed to establish a robust theoretical and predictive structure aimed at explaining the cosmological origin of the observed behavior. As we will show, our analysis presents—for the first time to the best of our knowledge—evidence for a transition from quintessence to phantom behavior at $z_{\dagger} \sim 0.5$, with a significance exceeding $\sim 5\sigma$.

This work is structured as follows: Sec. II presents the theoretical model and its main physical characteristics. Sec. IV describes the methodology and datasets employed in our analysis. The results are presented in Sec. V, and our final conclusions are summarized in Sec. VI.

II. AGNOSTIC TEST FOR PROBING LATE-TIME TRANSITIONS

We consider a homogeneous and isotropic model of the Universe, described by the Friedmann-Lemaître-Robertson-Walker (FLRW) metric, which serves as the foundation for modern cosmological models. The line element is given by:

$$ds^2 = -dt^2 + a^2(t) \left(\frac{dr^2}{1 - \kappa r^2} + r^2 d\theta^2 + r^2 \sin^2 \theta d\phi^2 \right), \quad (1)$$

where $a(t)$ is the scale factor governing the expansion of the Universe, and κ is the curvature parameter that determines the spatial geometry. Specifically, $\kappa = 0$ corresponds to a flat Universe, $\kappa > 0$ to a closed Universe with spherical spatial geometry, and $\kappa < 0$ to an open Universe with hyperbolic spatial curvature.

Since recent observations strongly support a spatially flat Universe, we adopt $\kappa = 0$ in our analysis. Under this assumption, the expansion rate of the Universe follows the Friedmann equation:

$$\mathcal{H}^2 = \frac{8\pi G}{3} a^2 \sum_i \rho_i, \quad (2)$$

where \mathcal{H} is the Hubble parameter in conformal time units, G is the gravitational constant, and the summation runs over all components i , including radiation (photons and neutrinos), baryons, cold dark matter (DM), and dark energy (DE). The total energy density consists of these four components, and we denote ρ_i as the energy density of the i -th component, where i runs over radiation (r), baryons (b), cold dark matter (c), and dark energy (x). Similarly, we denote p_i as the pressure of the i -th component.

The evolution of the DE energy density $\rho_x(z)$ depends on its equation of state (EoS). Assuming a constant w , the energy density evolves as:

$$\rho_x(z) = \rho_{x,0} (1 + z)^{3(1+w)}, \quad (3)$$

where $\rho_{x,0}$ is the present-day DE energy density. For $w = -1$, corresponding to a cosmological constant, $\rho_x(z)$ remains constant. However, deviations from this value indicate a dynamic behavior of DE.

In this work, we propose a general method—Independent of priors and initial theoretical assumptions—to test whether a transition in the dynamic nature of DE occurs at late times (characterized by a critical redshift z_{\dagger}) and to determine its direction (quintessence or phantom). Specifically, we propose that the EoS of DE undergoes an abrupt change, controlled by the parameter Δ at a critical scale factor a_{\dagger} , given by:

$$w(a) = -1 + \Delta \operatorname{sgn}[a_{\dagger} - a]. \quad (4)$$

To implement this approach systematically, we follow these steps:

- **Step 1:** Both the time of the transition described by Eq. (4), and the sign (and magnitude) of Δ remain free, to be determined solely by fitting the data during the Markov Chain Monte Carlo (MCMC) analysis.
- **Step 2:** Once the initial value of Δ is obtained, its sign is reversed at the critical scale factor a_{\dagger} .
- **Step 3:** The magnitude of the variation remains constant before and after the transition. In other words, the absolute value of Δ does not change; only its sign is reversed at the transition.

Figure 1 (left panel) shows the evolution of $w(a)$ undergoing an abrupt transition, illustrating the model's predictive behavior for different values of Δ and a_{\dagger} . This functional form enforces a piecewise behavior in which $w(a)$ shifts from $w = -1 + \Delta$ for $a < a_{\dagger}$ to $w = -1 - \Delta$ for $a > a_{\dagger}$. Here, Δ quantifies deviations from the cosmological constant, while a_{\dagger} denotes the transition epoch.

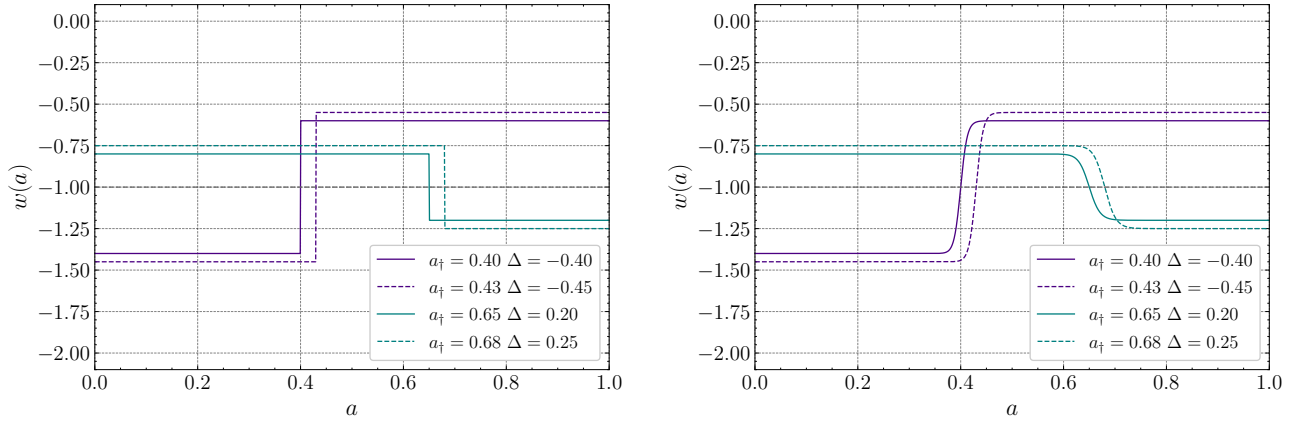


FIG. 1. Left panel: Evolution of $w(a)$ illustrating the abrupt transition for arbitrary values of a_f and Δ . Right panel: Smooth transition model Eq. (8) for arbitrary a_f and Δ , with $\zeta = 10^{1.5}$.

By treating Δ and a_f as free parameters—without imposing specific assumptions on the dynamics of dark energy—this framework provides an agnostic test for potential late-time transitions in the dark energy sector.

From the continuity equation, the DE energy density before the transition ($a < a_f$) follows:

$$\rho_x = \rho_{x,0} a^{-3\Delta} a_f^{6\Delta}, \quad (5)$$

where the standard solution is recovered for $a_f = 1$, implying no transition in the EoS.

Beyond altering the evolution of the cosmic background, a DE equation of state $w \neq -1$ also impacts the growth of perturbations. To analyze these effects, we work in the synchronous gauge, where the perturbed FLRW metric is given by

$$ds^2 = a^2(\eta) [-d\eta^2 + (\delta_{ij} + h_{ij})dx^i dx^j], \quad (6)$$

where $a(\eta)$ is the scale factor, η represents conformal time, and $h \equiv h_{ii}$ is the trace of the synchronous gauge metric perturbation h_{ij} . Transforming to Fourier space, we define the DE density contrast as δ_x and the velocity divergence as θ_x . Their evolution is governed by the following equations:

$$\begin{aligned} \dot{\delta}_x &= -(1+w) \left(\theta + \frac{h}{2} \right) - 3(\hat{c}_s^2 - w)\mathcal{H}\delta_x \\ &\quad - 9(1+w)(\hat{c}_s^2 - c_a^2)\mathcal{H}^2 \frac{\theta_x}{k^2}, \\ \dot{\theta}_x &= -(1-3\hat{c}_s^2)\mathcal{H}\theta_x + \frac{\hat{c}_s^2 k^2}{1+w}\delta_x - k^2\sigma_x. \end{aligned} \quad (7)$$

These equations are fully general, assuming a non-interacting fluid while allowing for the presence of shear stress σ_x , a non-adiabatic sound speed, and a time-dependent equation of state parameter w . From this point forward, we assume a shear-free fluid and adopt the parametrization of w given by Eq. (4). Within the perspectives discussed above, we adopt the PPF approximation [90] in all subsequent analyses.

III. EMBEDDING THE w -SWITCH MODEL WITHIN THE VCDM

The idea of a switch for the function $w(a)$ looks interesting, but from a theoretical point of view, one may wonder how to implement it so that the background evolution remains stable at all times. For instance, for a perfect fluid with pressure P and equation of state $P = P(\rho, s)$, s being the entropy per particle, we know that the perturbations propagate with a speed $c_s^2 = \left(\frac{\partial P}{\partial \rho} \right)_s$, see e.g. [91, 92]. On a homogeneous and isotropic background, this quantity would become $c_s^2 = P'/\rho' = w - \frac{1}{3}w'/(1+w)$, where a prime denotes differentiation with respect to the e-fold variable $N = \ln(a/a_0)$. Either before or after the sign-transition for w , since $w' \approx 0$, the value of c_s^2 would become negative, leading to an instability in the cosmological perturbations which would spoil the background dynamics in a time scale much shorter than the Hubble time. This shows that embedding this w -switch into a perfect fluid action is impossible.

However, there are theoretical models capable of embedding this w -switch without spoiling the results we want to present. In particular, we will show here the possibility of embedding the w -switch model into VCDM [88]. The theory of VCDM represents a model and framework that allows a large variety of time-dependent dark energy dynamics without introducing any new propagating gravity/matter degree of freedom. Doing so immediately implies that one does not need to worry about unstable or ghost-like degrees of freedom, just because they do not exist in the theory by construction. Several theoretical studies have been performed to understand this model, both in the context of compact objects and cosmology [89, 93–96], and other dark energy dynamical models have already been embedded in this framework [40, 45, 97]. Since the theoretical work has already been implemented elsewhere, here we just write down the two differences in the dynamics of background/perturbations

the model presents concerning Λ CDM. First, consider the background evolution: the w -transition must be smooth. To simplify the calculations, we adopt the following smooth functional form for $w(N)$:

$$w(N) = -1 + \Delta \tanh[\zeta(N_{\dagger} - N)] , \quad (8)$$

where ζ is the parameter that controls the rapidity and smoothness of the transition, and N is the e-fold time variable defined by $N = \ln(a/a_0)$, with $N \leq 0$. A larger ζ corresponds to a sharper transition, while a smaller ζ yields a more gradual change in $w(a)$. Figure 1 (right panel) shows the evolution of $w(a)$ under this approximation for the equation of state. With this choice, an analytical expression for ρ_x can be obtained, namely

$$\begin{aligned} \varrho_x &= C (\cosh[\zeta(N - N_{\dagger})])^{3\Delta/\zeta} \\ &= C \left[\frac{1}{2} \left(\frac{a}{a_{\dagger}} \right)^{\zeta} + \frac{1}{2} \left(\frac{a_{\dagger}}{a} \right)^{\zeta} \right]^{3\Delta/\zeta} , \end{aligned} \quad (9)$$

where C is a constant. Now the modified Friedmann equation reads

$$H(a)^2 = \sum_I \varrho_I(a) + \varrho_x(a) , \quad (10)$$

where H is the Hubble factor ($H = \dot{a}/a^2$ and a dot stands for derivative with respect to the conformal time), the index/label I runs over all the standard model matter components, and we have normalized for each matter component $\varrho = \rho/(3M_{\text{Pl}}^2)$. The constant C is determined by imposing $H_0^2(1 - \sum_I \Omega_{I0}) = \varrho_x(a = a_0)$. The pressure is given, by construction, by the expression $p_x = w \varrho_x$, here normalized, like the energy density, as $p_x = P_x/(3M_{\text{Pl}}^2)$.

The equations of motion for the cosmological perturbations, written here in the Newtonian gauge, are identical to those in the Λ CDM model (noting that VCDM does not introduce any additional perturbation modes), except for the momentum constraint, which can be expressed—without approximations—as

$$\dot{\Phi} + aH\Psi = \frac{3[k^2 - 3a^2(\dot{H}/a)]\sum_I(\varrho_I + p_I)\theta_I}{k^2[2k^2/a^2 + 9\sum_K(\varrho_K + p_K)]} , \quad (11)$$

where Φ and Ψ are the two Bardeen potentials, θ is the scalar perturbation of the fluid velocity, and, once more, the indices I and K run over all the standard model matter species (including the contribution from dark matter) except for the x -component. The difference here stands in the presence of the conformal time derivative of H , which differs from the expression valid in Λ CDM, i.e. $\dot{H}/a \neq -\frac{3}{2}\sum_I(\varrho_I + p_I)$.¹ Having stated the theory, we can proceed with the data analysis.

In what follows, we explore the observational constraints for both frameworks defined above, namely the $w_{\dagger}\text{CDM}$ and $w_{\dagger}\text{VCDM}$ models.

¹ The x -component does satisfy the continuity equation, $\dot{\varrho}_x/a = -3H(\varrho_x + p_x)$, but it is not a cosmological constant, $\varrho_x + p_x \neq 0$.

IV. DATASETS AND METHODOLOGY

To rigorously test our proposed theoretical framework, we implemented it within the Boltzmann solver **CLASS** [98] and performed Markov Chain Monte Carlo (MCMC) analyses using the publicly available sampler **MontePython** [99, 100]. Convergence was ensured in all runs by imposing the Gelman-Rubin criterion [101] with $R-1 \leq 10^{-2}$. We adopted flat priors on the cosmological parameter set $\{\Omega_b h^2, \Omega_c h^2, \tau_{\text{reio}}, 100\theta_s, \log(10^{10}A_s), n_s, \Delta, z_{\dagger}\}$, where the first six are standard Λ CDM parameters. Specifically, these include the present-day physical densities of baryons ($\omega_b = \Omega_b h^2$) and cold dark matter ($\omega_c = \Omega_c h^2$), the reionization optical depth (τ_{reio}), the angular scale of the sound horizon at recombination (θ_s), the amplitude of primordial scalar perturbations (A_s), and the spectral index of scalar fluctuations (n_s). The additional parameters Δ and z_{\dagger} characterize the transition in the dark energy equation of state. The prior ranges were set as follows: $\omega_b \in [0.0, 1.0]$, $\omega_{\text{cdm}} \in [0.0, 1.0]$, $100\theta_s \in [0.5, 2.0]$, $\log(10^{10}A_s) \in [1.0, 5.0]$, $n_s \in [0.1, 2.0]$, $\tau_{\text{reio}} \in [0.004, 0.8]$, $\Delta \in [-5, 5]$, and $z_{\dagger} \in [0, 10]$. For statistical analysis and visualization of the MCMC chains, we employed the Python package **GetDist**², which we used to derive 1D posterior distributions and 2D confidence contours.³

The datasets used in the analyses are described below.

- **Cosmic Microwave Background (CMB):** We utilize temperature and polarization anisotropy measurements of the CMB power spectra from the Planck satellite [2], along with their cross-spectra from the Planck 2018 legacy data release. Specifically, we employ the high- ℓ **Plik** likelihood for TT (in the multipole range $30 \leq \ell \leq 2508$), TE, and EE ($30 \leq \ell \leq 1996$), as well as the low- ℓ TT-only ($2 \leq \ell \leq 29$) likelihood and the low- ℓ EE-only ($2 \leq \ell \leq 29$) **SimA11** likelihood [3]. Additionally, we include CMB lensing measurements, which are reconstructed from the temperature 4-point correlation function [102]. We refer to this dataset as CMB.

- **Baryon Acoustic Oscillations (DESI DR2):** We consider BAO measurements from DESI’s second data release, which includes observations of galaxies and quasars [60], as well as Lyman- α tracers [103]. These measurements, detailed in Table IV of Ref. [60], cover both isotropic and anisotropic BAO constraints over $0.295 \leq z \leq 2.330$, divided into nine redshift bins. The BAO constraints are

² <https://github.com/cmbant/getdist>

³ Throughout this study, we expanded the prior ranges by up to an order of magnitude beyond the values reported here and those commonly used in standard analyses. We observed no significant impact on the results, confirming the robustness of our conclusions to the choice of prior ranges.

expressed in terms of the transverse comoving distance D_M/r_d , the Hubble horizon D_H/r_d , and the angle-averaged distance D_V/r_d , all normalized to the comoving sound horizon at the drag epoch, r_d . We also incorporate the correlation structure of these measurements through the cross-correlation coefficients: $r_{V,M/H}$, capturing the correlation between D_V/r_d and D_M/D_H , and $r_{M,H}$, which describes the correlation between D_M/r_d and D_H/r_d . This dataset is referred to as DR2.

- **Type Ia Supernovae (SN Ia):** Type Ia supernovae act as standardizable candles, providing a crucial method for measuring the universe's expansion history. Historically, SN Ia played a pivotal role in the discovery of the accelerating expansion of the universe [104, 105], building upon earlier, more complex arguments supporting Λ -dominated models from large-scale structure observations. In this work, we will use the following recent samples:

- (i) **PantheonPlus and Pantheon-Plus&SH0ES:** We integrated the latest distance modulus measurements from SN Ia in the PantheonPlus sample [106], which includes 1701 light curves from 1550 distinct SN Ia events, spanning a redshift range of 0.01 to 2.26. We designate this dataset as PP. Additionally, we consider a version of this sample that uses the latest SH0ES Cepheid host distance anchors [7] to calibrate the absolute magnitude of SN Ia, rather than centering a prior on the H_0 value from SH0ES. This approach allows for more robust results, and this version of the dataset is referred to as PPS.
- (ii) **Union 3.0:** The Union 3.0 compilation, consisting of 2087 SN Ia within the range $0.001 < z < 2.260$, was presented in [107]. Notably, 1363 of these SN Ia overlap with the PantheonPlus sample. This dataset features a distinct treatment of systematic errors and uncertainties, employing Bayesian Hierarchical Modeling. We refer to this dataset as Union3.
- (iii) **DESY5:** As part of their Year 5 data release, the Dark Energy Survey (DES) recently published results from a new, homogeneously selected sample of 1635 photometrically classified SN Ia with redshifts spanning $0.1 < z < 1.3$ [108]. This sample is complemented by 194 low-redshift SN Ia (shared with the PantheonPlus sample) in the range $0.025 < z < 0.1$. We refer to this dataset as DESY5.

A. Statistical tests and significance

When discussing the statistical significance of our model compared to the standard Λ CDM scenario, we

perform a chi-square difference test. Beyond this simple comparison, since the models in observational tests in this work have different numbers of free parameters, the standard model has $N_1 = 6$ free parameters. In contrast, our extended model introduces $N_2 = 8$, resulting in a difference in degrees of freedom $\Delta N = N_2 - N_1 = 2$. The difference in chi-square values, given by

$$\Delta\chi^2 = \chi^2_{\text{our model}} - \chi^2_{\Lambda\text{CDM}}, \quad (12)$$

follows a chi-square distribution with ΔN degrees of freedom, under the null hypothesis that the additional parameters do not improve the fit.

To determine the statistical significance, we compute the p -value, which is defined as the probability of obtaining a chi-square value greater than $|\Delta\chi^2|$. Then, to express this significance in terms of standard deviations, we use the inverse cumulative distribution function of the standard normal distribution, Φ^{-1} . The corresponding significance in terms of standard deviations, σ , is calculated as:

$$\sigma = \Phi^{-1} \left(1 - \frac{p}{2} \right), \quad (13)$$

where the factor $\frac{p}{2}$ accounts for the two-tailed significance test.

To further assess the level of agreement (or disagreement) between the models and their association with each analyzed dataset, we also perform a statistical comparison of the model with the Λ CDM scenario using the well-known Akaike Information Criterion (AIC) [109], defined as:

$$\text{AIC} \equiv -2 \ln L_{\max} + 2N, \quad (14)$$

where L_{\max} is the maximum likelihood of the model, and N is the total number of free parameters. A lower AIC value indicates a better model, balancing both goodness of fit and model complexity. Specifically, the AIC incorporates a penalty term for the number of parameters, discouraging the inclusion of unnecessary parameters that could lead to overfitting.

V. RESULTS AND DISCUSSIONS

In the discussions that follow, we will discuss and present our main results. We distinguish between the results obtained with and without the inclusion of DESI DR2 data. In each case, we consider two scenarios: the $w_{\dagger}\text{CDM}$ model and its generalization, the $w_{\dagger}\text{VCDM}$ model. For both models, we show the results for the key parameter of interest, primarily the deviation parameter Δ and its correlations with other cosmological parameters, such as H_0 and S_8 related to cosmic tensions. Additionally, we will present a detailed discussion about the statistical significance of our results relative to Λ CDM. Despite the structural generalization introduced

in w_{\dagger} VCDM, we find that its results remain broadly consistent with those of w_{\dagger} CDM. Therefore, given the strong similarity between the two cases, we will primarily refer to the w_{\dagger} CDM scenario in the following discussions, as the statistical conclusions are analogous for both models.

TABLE I. Marginalized constraints, along with the mean values at 68% CL, for both the free and some derived parameters of the models considered in this work, based on the CMB dataset and its combinations with PP&SH0ES. In the last rows, we present $\Delta\chi^2_{\min} = \chi^2_{\min}(\text{our model}) - \chi^2_{\min}(\Lambda\text{CDM})$ and $\Delta\text{AIC} = \text{AIC}_{\text{our model}} - \text{AIC}_{\Lambda\text{CDM}}$. Negative values for $\Delta\chi^2_{\min}$ and ΔAIC indicate a better fit of the model compared to the ΛCDM model.

Dataset	Planck	Planck+PP&SH0ES
Model	$w_{\dagger}\text{CDM}$	$w_{\dagger}\text{CDM}$
	$w_{\dagger}\text{VCDM}$	$w_{\dagger}\text{VCDM}$
$10^2\omega_b$	2.241 ± 0.016 2.246 ± 0.015	2.253 ± 0.014 2.255 ± 0.014
ω_{cdm}	0.1196 ± 0.0013 0.1190 ± 0.0012	0.1185 ± 0.0012 0.1183 ± 0.0012
$100\theta_s$	1.04189 ± 0.00030 1.04195 ± 0.00028	1.04205 ± 0.00030 1.04209 ± 0.00029
$\ln 10^{10} A_s$	3.042 ± 0.015 3.038 ± 0.014	3.050 ± 0.015 3.048 ± 0.015
n_s	0.9662 ± 0.0043 0.9677 ± 0.0039	0.9688 ± 0.0042 0.9694 ± 0.0041
τ_{reio}	0.0538 ± 0.0073 0.0527 ± 0.0072	$0.0582^{+0.0073}_{-0.0083}$ $0.0575^{+0.0069}_{-0.0083}$
Δ	$-0.29^{+0.24}_{-0.71}$ $-0.68^{+0.15}_{-0.28}$	-0.174 ± 0.054 -0.187 ± 0.051
z_{\dagger}	< 0.626 < 0.651	$0.167^{+0.036}_{-0.045}$ $0.174^{+0.032}_{-0.044}$
$H_0 [\text{km/s/Mpc}]$	$75.0^{+7.3}_{-13}$ $79.6^{+7.8}_{-9.0}$	69.93 ± 0.66 70.09 ± 0.66
Ω_m	$0.267^{+0.063}_{-0.079}$ $0.231^{+0.043}_{-0.053}$	0.2898 ± 0.0065 0.2882 ± 0.0064
S_8	$0.796^{+0.041}_{-0.030}$ $0.778^{+0.031}_{-0.027}$	0.801 ± 0.012 0.799 ± 0.012
$\Delta\chi^2_{\min}$	-3.90 -3.62	-12.78 -13.20
ΔAIC	0.10 0.38	-8.78 -9.20

In Table I, we first analyze the constraints imposed by CMB data alone and then explore its combination with the PP&SH0ES sample. Our findings show that CMB data by itself lacks sufficient sensitivity to constrain the extended parameter space of our models. In particular, it only provides an upper bound on the transition redshift, yielding $z_{\dagger} < 0.626$ at 68% CL. Likewise, the deviation parameter Δ remains weakly constrained, although there is a $\sim 1\sigma$ tendency toward deviations favoring $\Delta < 0$ in both scenarios. The presence of new degrees of freedom introduces degeneracies that reduce the con-

straining power of CMB data, especially in the estimation of H_0 and Ω_m . Although the posterior distributions of these parameters shift from their ΛCDM values, the associated uncertainties remain large. Consequently, the Planck-only dataset does not impose strong restrictions on the new physics explored by our frameworks.

Nonetheless, since the inferred values of H_0 from CMB only are in agreement with local measurements, we can reliably perform a joint analysis with the PP&SH0ES dataset. The addition of this late-time data significantly tightens the constraints on all cosmological parameters. We find $z_{\dagger} = 0.167^{+0.036}_{-0.045}$ and $\Delta = -0.174 \pm 0.054$ at 68% CL. These values indicate a departure from the ΛCDM dynamics, with a statistical preference for a late-time transition in the dark sector. The sign of $\Delta < 0$ implies that the dark energy equation of state transitions from a phantom-like regime at high redshifts to a quintessence regime at low redshifts. Moreover, the joint Planck+PP&SH0ES dataset yields $H_0 = 69.93 \pm 0.66$ km/s/Mpc, effectively reducing the Hubble tension to a moderate level. For this joint analysis, we find a chi-square difference of $\Delta\chi^2_{\min} = -12.78$, corresponding to a statistical significance of 3.1σ , and an AIC difference of $\Delta\text{AIC} = -8.78$. These results collectively support the existence of a transition in the dark energy dynamics at low redshift. The interpretation of the results using the w_{\dagger} VCDM model is equivalent to that discussed previously.

Figure 2 shows the marginalized one-dimensional posterior distributions and the 68% and 95% confidence level contours for the parameters Δ , H_0 , S_8 , and Ω_m for both models considered in this work. The analysis incorporates data from Planck+PP&SH0ES, Planck alone, and their combinations with DESI and several supernova samples, as indicated in the legend.

Now, let us focus on the joint analysis of Planck + DESI (see Table II). We obtain $\Delta = -0.226 \pm 0.070$ and $z_{\dagger} = 0.533 \pm 0.064$, which represents a significant deviation from the ΛCDM model, favoring $\Delta < 0$ at the 3.2σ level. The values of z_{\dagger} , as well as the overall parameter space of the model, are in tension with the Planck+PP&SH0ES sample, as the latter uses the latest SH0ES Cepheid host distance anchors to calibrate the absolute magnitude of SN Ia. Given this tension, we opted not to combine PP&SH0ES with DESI in our analysis. However, it is noteworthy that the overall dynamics favored by Planck+DESI align with those suggested by Planck+PP&SH0ES. For the joint Planck + DESI analysis, we note that $\Delta\text{AIC} = -10.18$, again favoring our extended model. Considering that in our model the present-day equation of state $w(z = 0)$ plays the same role as the w_0 parameter in the CPL parametrization, we can directly compare our predictions with those from DESI-DR2 [60]. In this case, we find $w(z = 0) = -0.774 \pm 0.070$, which is in relative good agreement with the DESI-DR2 constraint $w_0 = -0.42 \pm 0.21$ with in 1.6σ .

We now turn to an analysis incorporating additional SN Ia datasets. Currently, three major SN Ia samples

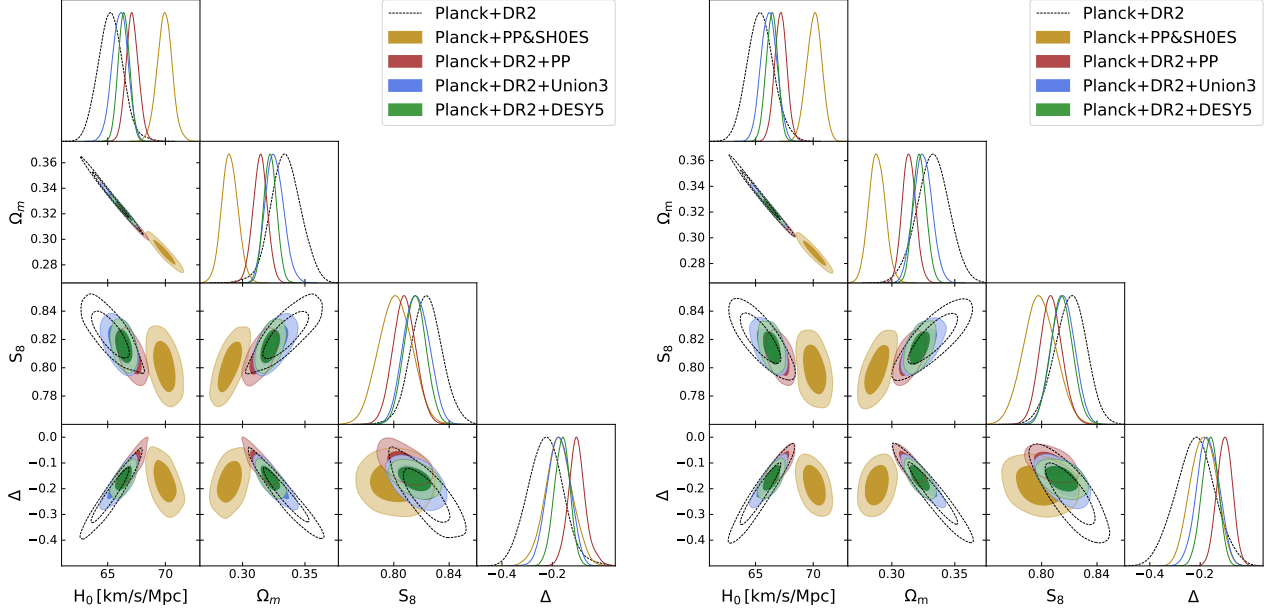


FIG. 2. Left panel: Marginalized one-dimensional posterior distributions and contours (68% and 95% CL) for the parameters Δ , H_0 , S_8 , and Ω_m in the w_t CDM model, based on the CMB dataset and its combinations with PP&SH0ES, DESI, PP, Union3, and DESY5, as indicated in the legend. Right panel: Same as the left panel, but for the w_t VCDM model.

are available: PantheonPlus (PP), Union3, and DESY5. In Table II, we summarize the results of combining each with Planck+DESI. These combinations consistently improve the parameter constraints and reinforce the statistical significance of a dynamical transition in the dark sector.

Let us first consider the combination Planck+DESI+PP. In this case, the inferred deviation parameter is $\Delta = -0.102^{+0.031}_{-0.035}$ with a transition redshift of $z_t = 0.553^{+0.047}_{-0.140}$, showing a mild but statistically significant departure from Λ CDM at the 2.9σ level ($\Delta\chi^2_{\min} = -11.44$, $\Delta\text{AIC} = -7.44$). These results are consistent with the dynamic displayed by Planck+PP&SH0ES, and strengthen the evidence for a late-time transition in the dark energy sector. The Hubble constant in this combination is constrained to $H_0 = 67.13 \pm 0.55$ km/s/Mpc, offering a partial alleviation of the H_0 tension, albeit not as strongly as with the inclusion of SH0ES calibration. In this case, our prediction for the present-day EoS is $w(z = 0) = -0.898^{+0.065}_{-0.031}$, which is in excellent agreement with the DESI-DR2 result, $w_0 = -0.838 \pm 0.055$ with 0.71σ .

Next, we analyze the Planck+DESI+Union3 combination. Here, we find $\Delta = -0.174 \pm 0.044$ and $z_t = 0.524 \pm 0.069$, favoring a dynamical transition at a significance level of 3.6σ ($\Delta\chi^2_{\min} = -14.86$, $\Delta\text{AIC} = -10.86$). Compared to the PP sample, Union3 supports a slightly more negative value of Δ , suggesting a more pronounced transition from phantom to quintessence behavior. The inferred Hubble constant is $H_0 = 66.06 \pm 0.68$ km/s/Mpc, consistent with intermediate redshift measurements and with slightly tighter constraints on $\Omega_m = 0.3256^{+0.0069}_{-0.0077}$.

These results further confirm the robustness of our model across multiple SN Ia datasets. The corresponding present-day EoS is $w(z = 0) = -0.826 \pm 0.044$ at 68% CL.

Finally, the most striking results are obtained when combining Planck+DESI+DESY5. In this case, we find the most significant statistical preference for our model: $\Delta = -0.162 \pm 0.031$ and $z_t = 0.490^{+0.063}_{-0.079}$, deviating from Λ CDM at the 4.9σ (5.1σ level, with $\Delta\chi^2_{\min} = -27.34$ -29.24) and $\Delta\text{AIC} = -23.34$. As highlighted in [110], a discrepancy of approximately 0.04 mag in magnitude between low and high redshifts was observed between the PP and DESY5 samples. This offset may partly explain the enhanced deviation seen in the DESY5 results. If the discrepancy is not due to systematic errors, it may point to genuine new physics in the dark sector, with our model capturing this late-time transition accurately. Lastly, the present-day EoS in this analysis predicts $w(z = 0) = -0.838 \pm 0.031$ at 68% CL.

As previously mentioned, all the analyses discussed above exhibit the same overall trends when interpreted within the w_t VCDM framework. It is important to highlight that the w_t VCDM model not only provides a slight improvement in the goodness of fit but also offers a solid theoretical foundation for the adopted parameterization. A major and noteworthy exception arises in the joint Planck+DESI+DESY5 analysis, where we observe an improvement at the level of approximately 5σ compared to the Λ CDM model. Such a high-significance result is particularly striking: in the context of statistical analyses, a 5σ detection is widely regarded as a robust threshold for a discovery-level claim. In Table III, we

TABLE II. Marginalized constraints, along with the mean values at 68% CL, for both the free and some derived parameters of the models considered in this work, based on the CMB dataset and its combinations with DESI, PPS, PP, Union3, and DESY5. In the last rows, we present $\Delta\chi^2_{\min} = \chi^2_{\min}(\text{our model}) - \chi^2_{\min}(\Lambda\text{CDM})$ and $\Delta\text{AIC} = \text{AIC}_{\text{our model}} - \text{AIC}_{\Lambda\text{CDM}}$. Negative values for $\Delta\chi^2_{\min}$ and ΔAIC indicate a better fit of the model compared to the ΛCDM model.

Dataset	Planck+DR2	Planck+DR2+PP	Planck+DR2+Union3	Planck+DR2+DESY5
Model	$w_{\dagger}\text{CDM}$ $w_{\dagger}\text{VCDM}$	$w_{\dagger}\text{CDM}$ $w_{\dagger}\text{VCDM}$	$w_{\dagger}\text{CDM}$ $w_{\dagger}\text{VCDM}$	$w_{\dagger}\text{CDM}$ $w_{\dagger}\text{VCDM}$
$10^2\omega_b$	2.241 ± 0.013 2.244 ± 0.013	2.249 ± 0.012 2.250 ± 0.012	2.245 ± 0.013 2.245 ± 0.012	2.245 ± 0.013 2.245 ± 0.012
ω_{cdm}	0.11929 ± 0.00070 $0.11922^{+0.00079}_{-0.00070}$	0.11836 ± 0.00058 0.11835 ± 0.00054	0.11893 ± 0.00060 0.11889 ± 0.00059	0.11892 ± 0.00056 0.11891 ± 0.00057
$100\theta_s$	1.04198 ± 0.00025 1.04196 ± 0.00027	1.04206 ± 0.00028 1.04205 ± 0.00027	1.04201 ± 0.00025 1.04199 ± 0.00027	1.04197 ± 0.00028 1.04200 ± 0.00027
$\ln 10^{10} A_s$	3.049 ± 0.013 3.045 ± 0.014	3.052 ± 0.015 $3.050^{+0.013}_{-0.015}$	$3.048^{+0.014}_{-0.017}$ 3.047 ± 0.014	3.049 ± 0.015 $3.046^{+0.013}_{-0.015}$
n_s	0.9672 ± 0.0032 0.9675 ± 0.0034	0.9692 ± 0.0033 0.9693 ± 0.0032	0.9677 ± 0.0033 0.9680 ± 0.0033	0.9678 ± 0.0032 0.9682 ± 0.0033
τ_{reio}	$0.0567^{+0.0059}_{-0.0068}$ $0.0555^{+0.0075}_{-0.0067}$	$0.0594^{+0.0067}_{-0.0077}$ $0.0584^{+0.0064}_{-0.0077}$	$0.0567^{+0.0065}_{-0.0079}$ 0.0566 ± 0.0069	0.0573 ± 0.0071 $0.0561^{+0.0066}_{-0.0074}$
Δ	-0.226 ± 0.070 -0.220 ± 0.077	$-0.102^{+0.031}_{-0.035}$ -0.103 ± 0.031	-0.174 ± 0.044 -0.169 ± 0.043	-0.162 ± 0.031 -0.161 ± 0.033
z_{\dagger}	0.533 ± 0.064 $0.521^{+0.057}_{-0.052}$	$0.553^{+0.047}_{-0.140}$ 0.504 ± 0.095	0.524 ± 0.069 0.519 ± 0.067	$0.490^{+0.063}_{-0.079}$ $0.493^{+0.063}_{-0.081}$
H_0 [km/s/Mpc]	65.3 ± 1.1 65.4 ± 1.1	67.13 ± 0.55 67.18 ± 0.53	66.06 ± 0.68 66.16 ± 0.68	66.40 ± 0.49 66.41 ± 0.50
Ω_m	0.335 ± 0.012 0.333 ± 0.013	0.3141 ± 0.0058 0.3136 ± 0.0054	$0.3256^{+0.0069}_{-0.0077}$ 0.3245 ± 0.0073	0.3222 ± 0.0051 0.3220 ± 0.0053
S_8	0.824 ± 0.011 $0.821^{+0.012}_{-0.011}$	0.8077 ± 0.0083 0.8068 ± 0.0080	0.8163 ± 0.0090 0.8153 ± 0.0084	0.8154 ± 0.0079 0.8145 ± 0.0079
$\Delta\chi^2_{\min}$	-10.18 -12.40	-11.44 -11.40	-14.86 -16.36	-27.34 -29.24
ΔAIC	-6.18 -8.40	-7.44 -7.40	-10.86 -12.36	-23.34 -25.24

summarize the statistical significance of the results for both models across all analyses conducted in this study. Therefore, this deviation represents a substantial challenge to the dynamics predicted by the standard ΛCDM cosmological model, potentially signaling the need for extensions or modifications to the standard framework.

Figure 3 illustrates the evolution of the dark energy equation of state and the normalized energy density as functions of redshift. As seen in the left panel, the equation of state evolves from a phantom-like regime

($w < -1$) at early times to a quintessence-like regime ($w > -1$) today. This behavior is driven by the negative Δ values inferred from all dataset combinations. Interestingly, this evolving behavior of the EoS is consistent with the trends reported in the latest DESI collaboration results [60], which also favor a dynamic dark energy scenario transitioning from phantom to quintessence. Moreover, the redshift at which this transition occurs in our model, lies within the same range indicated by DESI's findings—see Fig. 12 in Ref. [60], around $z \sim 0.3\text{--}0.5$.

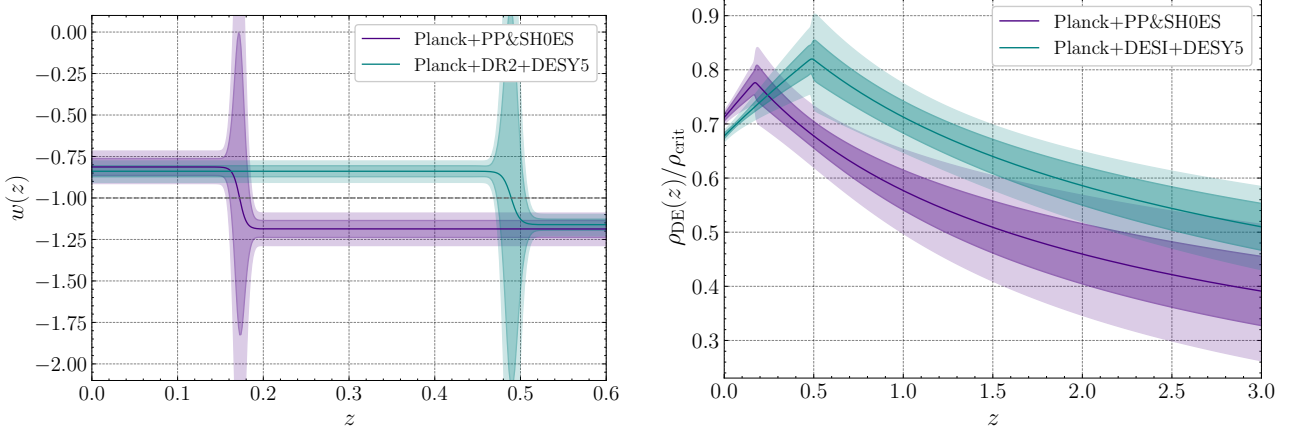


FIG. 3. Left panel: Statistical reconstruction of the dark energy equation of state at 1σ and 2σ confidence levels based on the joint analyses of Planck + PP&SH0ES and Planck + DESI + DESY5 data. The evolution shows a transition from a phantom-like regime ($w < -1$) at early times to a quintessence-like regime ($w > -1$) today, driven by the negative values of the deviation parameter Δ . Right panel: Evolution of the normalized dark energy density, $\rho_{\text{DE}}/\rho_{\text{crit}}$, for the best-fit solutions from the same datasets. The plot highlights how the change in the deviation parameter affects the scaling of dark energy relative to the critical density at late times.

It is important to note that near the transition redshift, the rapid change predicted by the model leads to a significant amplification of error propagation within this interval. This effect does not impact the best-fit value itself but becomes evident when reconstructing the confidence regions, as it stems from the calculation of partial derivatives used in the statistical reconstruction of functions. In other words, this behavior arises purely from numerical effects associated with the sharp transition in the equation of state. The right panel complements this phenomenology by showing the impact of the transition on the background evolution, highlighting how the dark energy density tracks the critical density differently across epochs.

Although our model consistently yields a better fit to the data than the standard Λ CDM scenario—particularly in combinations involving DESY5 and PP&SH0ES—it is important to emphasize that it neither resolves the H_0 tension nor substantially mitigates the S_8 discrepancy. As shown in Table III, the improvement in fit is statistically significant across all datasets, reaching the $\sim 5\sigma$ level in the Planck+DESI+DESY5 analysis. Nevertheless, even in this best-fit case, the derived value of $H_0 = 66.40 \pm 0.49$ km/s/Mpc remains in tension with local determinations of H_0 , although it is in remarkable agreement with the DESI-DR2 prediction of $H_0 = 66.74 \pm 0.56$ km/s/Mpc for the $w_0 w_a$ CDM model. This indicates that, while the model introduces a robust and theoretically well-motivated modification to the late-time behavior of dark energy—characterized by a transition from a phantom-like to a quintessence regime—it does not fully resolve all existing cosmological tensions.

$w_0 w_a$ CDM	$\Delta\chi^2_{\text{min}}$	Statistical significance σ
Planck	-3.90	1.5
	-3.62	1.4
Planck + DR2	-10.18	2.7
	-12.40	3.1
Planck + DR2 + PP	-11.44	2.9
	-11.40	2.9
Planck + PP&SH0ES	-12.78	3.1
	-13.20	3.2
Planck + DR2 + Union3	-14.86	3.4
	-16.36	3.6
Planck + DR2 + DESY5	-27.34	4.9
	-29.24	5.1

TABLE III. Statistical significance in favor of a transition from a phantom-like phase to a quintessence regime at late times, relative to the Λ CDM model.

VI. CONCLUSIONS

In this work, we have investigated an extension of the standard Λ CDM model that incorporates a late-time dynamical transition in the dark energy sector. This extended scenario introduces two additional parameters: the deviation parameter Δ , which quantifies the depar-

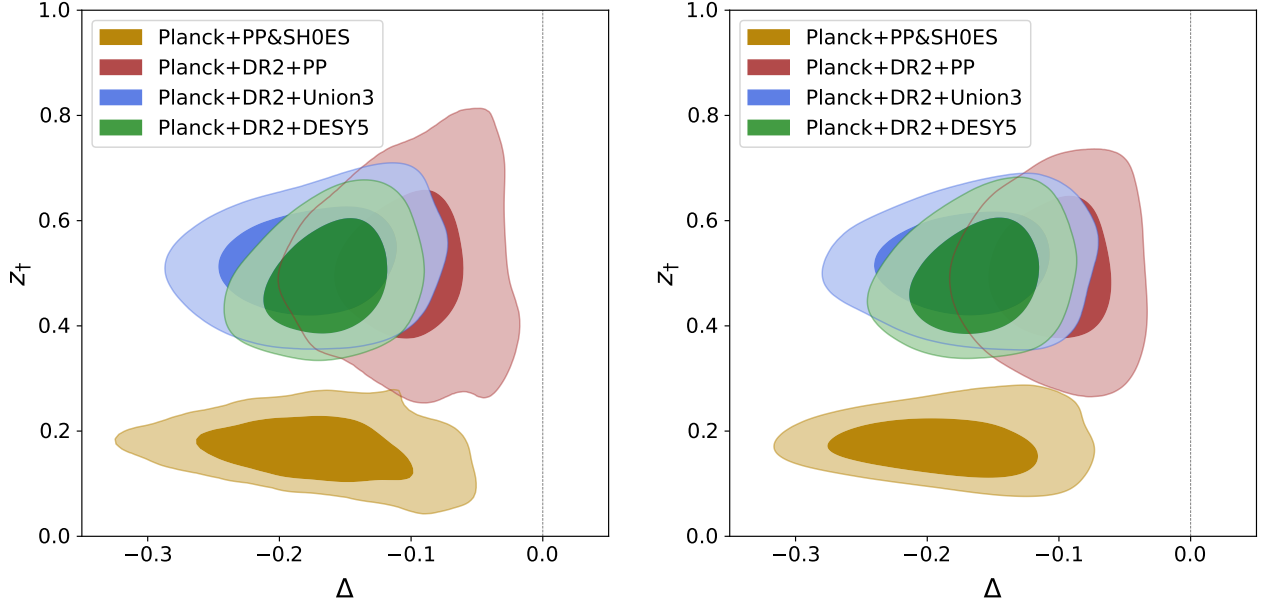


FIG. 4. Left panel: The 2D contours at 68% and 95% confidence levels for the parameters $\Delta-z_{\dagger}$ are obtained from different data combinations, as indicated in the legend, in the w_{\dagger} CDM model. Right panel: Same as the left panel, but for the w_{\dagger} VCDM model.

ture from a cosmological constant behavior, and the transition redshift z_{\dagger} , marking the epoch at which the dark energy equation of state undergoes a transition—left unconstrained a priori and determined directly from the data. Through a comprehensive statistical analysis, we tested the observational viability of this model using multiple datasets, including CMB measurements from Planck, BAO data from DESI, and three independent SN Ia compilations (PantheonPlus, Union3, and DESY5), along with the locally calibrated PP&SH0ES sample.

Our main findings can be summarized as follows:

- **Model Selection and Significance:** The extended model consistently provides better fits than the standard Λ CDM scenario, exhibiting statistically significant improvements in both χ^2 and AIC values. Across all dataset combinations, the $\Delta\chi^2$ values are negative and substantial, reaching as low as -29.24 for the Planck+DESI+DESY5 combination. This corresponds to a statistical preference of $\sim 5\sigma$ in favor of the extended models.
- **Consistency Across Datasets:** The values inferred for Δ and z_{\dagger} are consistent across different dataset combinations, with all analyses favoring $\Delta < 0$ and $z_{\dagger} \sim 0.3-0.5$. These results suggest a coherent picture in which the DE component exhibits phantom-like behavior at high redshifts and transitions to a quintessence-like phase at low redshifts.
- **Impact on Cosmological Tensions:** The extended model results in only moderately higher values of H_0 . For example, the Planck+PP&SH0ES combi-

nation yields $H_0 = 69.93 \pm 0.66$ km/s/Mpc, leading to a partial reduction of the Hubble tension but falling short of fully resolving it. Thus, while the model alleviates the discrepancy to some extent, it does not provide a satisfactory explanation for the H_0 tension.

- **Role of Supernova Samples (see Figure 4):** Among the SN Ia datasets considered, the DESY5 sample provides the strongest statistical support for a dynamical transition in the dark sector. The enhanced deviation observed in this dataset, compared to PantheonPlus and Union3, suggests a possible signature of new physics. This strengthens the case for our proposed extension. Figure 4 displays the 2D confidence contours at 68% and 95% CL in the $\Delta-z_{\dagger}$ plane, highlighting the distinct role played by the different supernova samples.

Our results open new avenues for exploring the nature of dark energy beyond the cosmological constant paradigm, as our analyses reveal deviations from the Λ CDM model at a significance level of approximately 5σ . Notably, the inferred redshift range for the transition lies well within the observational capabilities of current surveys, such as DESI. While improved observational constraints will be crucial, future theoretical efforts should also focus on linking the phenomenological behavior uncovered in this work to specific microphysical mechanisms. Embedding this effective description within a more fundamental theoretical framework would further strengthen its status as a physically motivated extension of the standard cosmological model.

ACKNOWLEDGMENTS

M.S. and M.A.S received support from the CAPES scholarship. R.C.N. thanks the financial support from the Conselho Nacional de Desenvolvimento Científico

e Tecnológico (CNPq, National Council for Scientific and Technological Development) under the project No. 304306/2022-3, and the Fundação de Amparo à Pesquisa do Estado do RS (FAPERGS, Research Support Foundation of the State of RS) for partial financial support under the project No. 23/2551-0000848-3.

[1] N. Aghanim *et al.* (Planck), *Astron. Astrophys.* **641**, A1 (2020), [arXiv:1807.06205](https://arxiv.org/abs/1807.06205) [astro-ph.CO].

[2] N. Aghanim *et al.* (Planck), *Astron. Astrophys.* **641**, A6 (2020), [Erratum: *Astron. Astrophys.* 652, C4 (2021)], [arXiv:1807.06209](https://arxiv.org/abs/1807.06209) [astro-ph.CO].

[3] N. Aghanim *et al.* (Planck), *Astron. Astrophys.* **641**, A5 (2020), [arXiv:1907.12875](https://arxiv.org/abs/1907.12875) [astro-ph.CO].

[4] V. Mossa *et al.*, *Nature* **587**, 210 (2020).

[5] S. Aiola *et al.* (ACT), *JCAP* **12**, 047 (2020), [arXiv:2007.07288](https://arxiv.org/abs/2007.07288) [astro-ph.CO].

[6] S. Alam *et al.* (eBOSS), *Phys. Rev. D* **103**, 083533 (2021), [arXiv:2007.08991](https://arxiv.org/abs/2007.08991) [astro-ph.CO].

[7] A. G. Riess *et al.*, *Astrophys. J. Lett.* **934**, L7 (2022), [arXiv:2112.04510](https://arxiv.org/abs/2112.04510) [astro-ph.CO].

[8] M. Kamionkowski and A. G. Riess, *Ann. Rev. Nucl. Part. Sci.* **73**, 153 (2023), [arXiv:2211.04492](https://arxiv.org/abs/2211.04492) [astro-ph.CO].

[9] L. Verde, N. Schöneberg, and H. Gil-Marín, (2023), [arXiv:2311.13305](https://arxiv.org/abs/2311.13305) [astro-ph.CO].

[10] E. Di Valentino and D. Brout, eds., *The Hubble Constant Tension*, Springer Series in Astrophysics and Cosmology (Springer, 2024).

[11] L. Breuval, A. G. Riess, S. Casertano, W. Yuan, L. M. Macri, M. Romaniello, Y. S. Murakami, D. Scolnic, G. S. Anand, and I. Soszyński, (2024), [arXiv:2404.08038](https://arxiv.org/abs/2404.08038) [astro-ph.CO].

[12] S. Li, A. G. Riess, S. Casertano, G. S. Anand, D. M. Scolnic, W. Yuan, L. Breuval, and C. D. Huang, *Astrophys. J.* **966**, 20 (2024), [arXiv:2401.04777](https://arxiv.org/abs/2401.04777) [astro-ph.CO].

[13] Y. S. Murakami, A. G. Riess, B. E. Stahl, W. D. Kenworthy, D.-M. A. Pluck, A. Macoretti, D. Brout, D. O. Jones, D. M. Scolnic, and A. V. Filippenko, *JCAP* **11**, 046 (2023), [arXiv:2306.00070](https://arxiv.org/abs/2306.00070) [astro-ph.CO].

[14] L. Verde, T. Treu, and A. G. Riess, *Nature Astron.* **3**, 891 (2019), [arXiv:1907.10625](https://arxiv.org/abs/1907.10625) [astro-ph.CO].

[15] L. Knox and M. Millea, *Phys. Rev. D* **101**, 043533 (2020), [arXiv:1908.03663](https://arxiv.org/abs/1908.03663) [astro-ph.CO].

[16] E. Di Valentino *et al.*, *Astropart. Phys.* **131**, 102605 (2021), [arXiv:2008.11284](https://arxiv.org/abs/2008.11284) [astro-ph.CO].

[17] E. Di Valentino, O. Mena, S. Pan, L. Visinelli, W. Yang, A. Melchiorri, D. F. Mota, A. G. Riess, and J. Silk, *Class. Quant. Grav.* **38**, 153001 (2021), [arXiv:2103.01183](https://arxiv.org/abs/2103.01183) [astro-ph.CO].

[18] E. Di Valentino, *Universe* **8**, 399 (2022).

[19] K. Said *et al.*, (2024), [arXiv:2408.13842](https://arxiv.org/abs/2408.13842) [astro-ph.CO].

[20] P. Boubel, M. Colless, K. Said, and L. Staveley-Smith, *Mon. Not. Roy. Astron. Soc.* **533**, 1550 (2024), [arXiv:2408.03660](https://arxiv.org/abs/2408.03660) [astro-ph.CO].

[21] W. L. Freedman, B. F. Madore, I. S. Jang, T. J. Hoyt, A. J. Lee, and K. A. Owens, (2024), [arXiv:2408.06153](https://arxiv.org/abs/2408.06153) [astro-ph.CO].

[22] A. G. Riess *et al.*, (2024), [arXiv:2408.11770](https://arxiv.org/abs/2408.11770) [astro-ph.CO].

[23] D. Scolnic *et al.*, (2024), [arXiv:2409.14546](https://arxiv.org/abs/2409.14546) [astro-ph.CO].

[24] M. Asgari *et al.* (KiDS), *Astron. Astrophys.* **645**, A104 (2021), [arXiv:2007.15633](https://arxiv.org/abs/2007.15633) [astro-ph.CO].

[25] M. A. Troxel *et al.* (DES), *Phys. Rev. D* **98**, 043528 (2018), [arXiv:1708.01538](https://arxiv.org/abs/1708.01538) [astro-ph.CO].

[26] A. H. Wright *et al.*, (2025), [arXiv:2503.19441](https://arxiv.org/abs/2503.19441) [astro-ph.CO].

[27] B. Stözlner *et al.*, (2025), [arXiv:2503.19442](https://arxiv.org/abs/2503.19442) [astro-ph.CO].

[28] T. Louis *et al.* (ACT), (2025), [arXiv:2503.14452](https://arxiv.org/abs/2503.14452) [astro-ph.CO].

[29] N. Sailer *et al.*, (2024), [arXiv:2407.04607](https://arxiv.org/abs/2407.04607) [astro-ph.CO].

[30] S. Chen *et al.*, (2024), [arXiv:2407.04795](https://arxiv.org/abs/2407.04795) [astro-ph.CO].

[31] D. Anbagajane *et al.*, (2025), [arXiv:2502.17677](https://arxiv.org/abs/2502.17677) [astro-ph.CO].

[32] C. García-García, M. Zennaro, G. Aricò, D. Alonso, and R. E. Angulo, *JCAP* **08**, 024 (2024), [arXiv:2403.13794](https://arxiv.org/abs/2403.13794) [astro-ph.CO].

[33] S. Sugiyama *et al.*, *Phys. Rev. D* **108**, 123521 (2023), [arXiv:2304.00705](https://arxiv.org/abs/2304.00705) [astro-ph.CO].

[34] M. M. Ivanov, A. Obuljen, C. Cuesta-Lazaro, and M. W. Toomey, (2024), [arXiv:2409.10609](https://arxiv.org/abs/2409.10609) [astro-ph.CO].

[35] S.-F. Chen, M. M. Ivanov, O. H. E. Philcox, and L. Wenzl, (2024), [arXiv:2406.13388](https://arxiv.org/abs/2406.13388) [astro-ph.CO].

[36] R. C. Nunes and S. Vagnozzi, *Mon. Not. Roy. Astron. Soc.* **505**, 5427 (2021), [arXiv:2106.01208](https://arxiv.org/abs/2106.01208) [astro-ph.CO].

[37] L. Kazantzidis and L. Perivolaropoulos, *Phys. Rev. D* **97**, 103503 (2018), [arXiv:1803.01337](https://arxiv.org/abs/1803.01337) [astro-ph.CO].

[38] T. Karim *et al.*, *JCAP* **02**, 045 (2025), [arXiv:2408.15909](https://arxiv.org/abs/2408.15909) [astro-ph.CO].

[39] R. Dalal *et al.*, *Phys. Rev. D* **108**, 123519 (2023), [arXiv:2304.00701](https://arxiv.org/abs/2304.00701) [astro-ph.CO].

[40] E. Di Valentino *et al.*, (2025), [arXiv:2504.01669](https://arxiv.org/abs/2504.01669) [astro-ph.CO].

[41] O. Akarsu, E. Di Valentino, S. Kumar, R. C. Nunes, J. A. Vazquez, and A. Yadav, (2023), [arXiv:2307.10899](https://arxiv.org/abs/2307.10899) [astro-ph.CO].

[42] J. F. Sorianio, S. Wohlberg, and L. A. Anchordoqui, (2025), [arXiv:2502.19239](https://arxiv.org/abs/2502.19239) [astro-ph.CO].

[43] M. S. Souza, A. M. Barcelos, R. C. Nunes, O. Akarsu, and S. Kumar, *Universe* **11**, 2 (2025), [arXiv:2501.18031](https://arxiv.org/abs/2501.18031) [astro-ph.CO].

[44] A. Gómez-Valent and J. Solà Peracaula, *Phys. Lett. B* **864**, 139391 (2025), [arXiv:2412.15124](https://arxiv.org/abs/2412.15124) [astro-ph.CO].

[45] O. Akarsu, A. De Felice, E. Di Valentino, S. Kumar, R. C. Nunes, E. Özülker, J. A. Vazquez, and A. Yadav, *Phys. Rev. D* **110**, 103527 (2024), [arXiv:2406.07526](https://arxiv.org/abs/2406.07526) [astro-ph.CO].

[46] E. Di Valentino, R. Z. Ferreira, L. Visinelli, and U. Danielsson, *Phys. Dark Univ.* **26**, 100385 (2019),

arXiv:1906.11255 [astro-ph.CO].

[47] J.-P. Hu and F. Y. Wang, *Mon. Not. Roy. Astron. Soc.* **517**, 576 (2022), arXiv:2203.13037 [astro-ph.CO].

[48] P. Mukherjee, K. F. Dialektopoulos, J. Levi Said, and J. Mifsud, *JCAP* **09**, 060 (2024), arXiv:2402.10502 [astro-ph.CO].

[49] G. Alestas, L. Perivolaropoulos, and K. Tanidis, *Phys. Rev. D* **106**, 023526 (2022), arXiv:2201.05846 [astro-ph.CO].

[50] S. Tsujikawa and M. Sami, *JCAP* **01**, 006 (2007), arXiv:hep-th/0608178.

[51] B. A. Bassett, M. Kunz, J. Silk, and C. Ungarelli, *Mon. Not. Roy. Astron. Soc.* **336**, 1217 (2002), arXiv:astro-ph/0203383.

[52] C. J. A. P. Martins and M. P. Colomer, *Astron. Astrophys.* **616**, A32 (2018), arXiv:1806.07653 [astro-ph.CO].

[53] M. A. Sabogal, E. Silva, R. C. Nunes, S. Kumar, and E. Di Valentino, *Phys. Rev. D* **111**, 043531 (2025), arXiv:2501.10323 [astro-ph.CO].

[54] G. Alestas, D. Camarena, E. Di Valentino, L. Kazantzidis, V. Marra, S. Nesseris, and L. Perivolaropoulos, *Phys. Rev. D* **105**, 063538 (2022), arXiv:2110.04336 [astro-ph.CO].

[55] Y. Liu, H. Yu, and P. Wu, *Phys. Rev. D* **110**, L021304 (2024), arXiv:2406.02956 [astro-ph.CO].

[56] S. Vagnozzi, *Universe* **9**, 393 (2023), arXiv:2308.16628 [astro-ph.CO].

[57] L. Huang, S.-J. Wang, and W.-W. Yu, *Sci. China Phys. Mech. Astron.* **68**, 220413 (2025), arXiv:2401.14170 [astro-ph.CO].

[58] M. A. Karim *et al.* (DESI), (2025), arXiv:2503.14745 [astro-ph.CO].

[59] A. G. Adame *et al.* (DESI), *Astron. J.* **168**, 58 (2024), arXiv:2306.06308 [astro-ph.CO].

[60] M. A. Karim *et al.* (DESI), (2025), arXiv:2503.14738 [astro-ph.CO].

[61] A. G. Adame *et al.* (DESI), (2024), arXiv:2404.03002 [astro-ph.CO].

[62] K. Lodha *et al.* (DESI), (2025), arXiv:2503.14743 [astro-ph.CO].

[63] R. Calderon *et al.* (DESI), *JCAP* **10**, 048 (2024), arXiv:2405.04216 [astro-ph.CO].

[64] A. G. Adame *et al.* (DESI), (2024), arXiv:2411.12022 [astro-ph.CO].

[65] M. Ishak *et al.*, (2024), arXiv:2411.12026 [astro-ph.CO].

[66] W. Elbers *et al.* (DESI), (2025), arXiv:2503.14744 [astro-ph.CO].

[67] K. Lodha *et al.* (DESI), *Phys. Rev. D* **111**, 023532 (2025), arXiv:2405.13588 [astro-ph.CO].

[68] E. Silva, M. A. Sabogal, M. S. Souza, R. C. Nunes, E. Di Valentino, and S. Kumar, (2025), arXiv:2503.23225 [astro-ph.CO].

[69] R. Shah, P. Mukherjee, and S. Pal, (2025), arXiv:2503.21652 [astro-ph.CO].

[70] Y.-H. Pang, X. Zhang, and Q.-G. Huang, (2025), arXiv:2503.21600 [astro-ph.CO].

[71] A. Paliathanasis, (2025), arXiv:2503.20896 [astro-ph.CO].

[72] S. Hur, V. Jejjala, M. J. Kavic, D. Minic, and T. Takeuchi, (2025), arXiv:2503.20854 [hep-th].

[73] L. A. Ureña López *et al.* (DESI), (2025), arXiv:2503.20178 [astro-ph.CO].

[74] L. A. Anchordoqui, I. Antoniadis, and D. Lust, (2025), arXiv:2503.19428 [hep-th].

[75] J. Pan and G. Ye, (2025), arXiv:2503.19898 [astro-ph.CO].

[76] J.-Q. Jiang, W. Giarè, S. Gariazzo, M. G. Dainotti, E. Di Valentino, O. Mena, D. Pedrotti, S. S. da Costa, and S. Vagnozzi, (2024), arXiv:2407.18047 [astro-ph.CO].

[77] J.-Q. Jiang, D. Pedrotti, S. S. da Costa, and S. Vagnozzi, (2024), arXiv:2408.02365 [astro-ph.CO].

[78] A. Chakraborty, P. K. Chanda, S. Das, and K. Dutta, (2025), arXiv:2503.10806 [astro-ph.CO].

[79] S. Pan, S. Paul, E. N. Saridakis, and W. Yang, (2025), arXiv:2504.00994 [astro-ph.CO].

[80] C. You, D. Wang, and T. Yang, (2025), arXiv:2504.00985 [astro-ph.CO].

[81] S. Afroz and S. Mukherjee, (2025), arXiv:2504.16868 [astro-ph.CO].

[82] D. Wang, (2025), arXiv:2504.15635 [astro-ph.CO].

[83] P. Adolf, M. Hirsch, S. Krieg, H. Päs, and M. Tabet, (2025), arXiv:2504.15332 [astro-ph.CO].

[84] B. R. Dinda and R. Maartens, (2025), arXiv:2504.15190 [astro-ph.CO].

[85] U. Kumar, A. Ajith, and A. Verma, (2025), arXiv:2504.14419 [astro-ph.CO].

[86] W. Giarè, T. Mahassen, E. Di Valentino, and S. Pan, *Phys. Dark Univ.* **48**, 101906 (2025), arXiv:2502.10264 [astro-ph.CO].

[87] E. M. Teixeira, W. Giarè, N. B. Hogg, T. Montandon, A. Poudou, and V. Poulin, (2025), arXiv:2504.10464 [astro-ph.CO].

[88] A. De Felice, A. Doll, and S. Mukohyama, *JCAP* **09**, 034 (2020), arXiv:2004.12549 [gr-qc].

[89] A. De Felice, S. Mukohyama, and M. C. Pookkillath, *Phys. Lett. B* **816**, 136201 (2021), [Erratum: *Phys. Lett. B* 818, 136364 (2021)], arXiv:2009.08718 [astro-ph.CO].

[90] W. Fang, W. Hu, and A. Lewis, *Phys. Rev. D* **78**, 087303 (2008), arXiv:0808.3125 [astro-ph].

[91] C. W. Misner, K. S. Thorne, and J. A. Wheeler, *Gravitation* (W. H. Freeman, San Francisco, 1973).

[92] A. De Felice, J.-M. Gerard, and T. Suyama, *Phys. Rev. D* **81**, 063527 (2010), arXiv:0908.3439 [gr-qc].

[93] A. De Felice, S. Mukohyama, and M. C. Pookkillath, *Phys. Rev. D* **105**, 104013 (2022), arXiv:2110.14496 [gr-qc].

[94] A. De Felice, K.-i. Maeda, S. Mukohyama, and M. C. Pookkillath, *JCAP* **03**, 030 (2023), arXiv:2211.14760 [gr-qc].

[95] A. F. Jalali, P. Martens, and S. Mukohyama, *Phys. Rev. D* **109**, 044053 (2024), arXiv:2306.10672 [gr-qc].

[96] A. De Felice, K.-i. Maeda, S. Mukohyama, and M. C. Pookkillath, *Phys. Rev. D* **106**, 024028 (2022), arXiv:2204.08294 [gr-qc].

[97] O. Akarsu, A. De Felice, E. Di Valentino, S. Kumar, R. C. Nunes, E. Ozulker, J. A. Vazquez, and A. Yadav, (2024), arXiv:2402.07716 [astro-ph.CO].

[98] D. Blas, J. Lesgourges, and T. Tram, *JCAP* **07**, 034 (2011), arXiv:1104.2933 [astro-ph.CO].

[99] T. Brinckmann and J. Lesgourges, *Phys. Dark Univ.* **24**, 100260 (2019), arXiv:1804.07261 [astro-ph.CO].

[100] B. Audren, J. Lesgourges, K. Benabed, and S. Prunet, *JCAP* **02**, 001 (2013), arXiv:1210.7183 [astro-ph.CO].

[101] A. Gelman and D. B. Rubin, *Statist. Sci.* **7**, 457 (1992).

[102] N. Aghanim *et al.* (Planck), *Astron. Astrophys.* **641**, A8 (2020), arXiv:1807.06210 [astro-ph.CO].

- [103] M. Abdul Karim *et al.* (DESI), (2025), arXiv:2503.14739 [astro-ph.CO].
- [104] A. G. Riess *et al.* (Supernova Search Team), *Astron. J.* **116**, 1009 (1998), arXiv:astro-ph/9805201.
- [105] S. Perlmutter *et al.* (Supernova Cosmology Project), *Astrophys. J.* **517**, 565 (1999), arXiv:astro-ph/9812133.
- [106] D. Brout *et al.*, *Astrophys. J.* **938**, 110 (2022), arXiv:2202.04077 [astro-ph.CO].
- [107] D. Rubin *et al.*, (2023), arXiv:2311.12098 [astro-ph.CO].
- [108] T. M. C. Abbott *et al.* (DES), (2024), arXiv:2401.02929 [astro-ph.CO].
- [109] H. Akaike, *IEEE Trans. Automatic Control* **19**, 716 (1974).
- [110] G. Efstathiou, (2024), arXiv:2408.07175 [astro-ph.CO].